Accepted for publication in AJ
Preprint typeset using LATEX style emulateapj v. 10/09/06

arXiv:0801.1111v1 [astro-ph] 7 Jan 2008

AN ACCURATE AGE DETERMINATION FOR THE SMC STAR CLUSTER NGC 121 WITH HST/ACS [*]

Katharina Glatt[1,2,3], John S. Gallagher III.[2], Eva K. Grebel[1,3], Antonella Nota[4], Elena Sabbi[4], Marco Sirianni[4], Gisella Clementini[5], Monica Tosi[5], Daniel Harbeck[2], Andreas Koch[1,6], and Misty Cracraft[4]

Accepted for publication in AJ

ABSTRACT

As first Paper of a series devoted to study the old stellar population in clusters and fields in the Small Magellanic Cloud, we present deep observations of NGC 121 in the F555W and F814W filters, obtained with the Advanced Camera for Surveys on the *Hubble Space Telescope*. The resulting color-magnitude diagram reaches ~ 3.5 mag below the main-sequence turn-off; deeper than any previous data. We derive the age of NGC 121 using both absolute and relative age-dating methods. Fitting isochrones in the ACS photometric system to the observed ridge line of NGC 121, gives ages of 11.8 ± 0.5 Gyr (Teramo), 11.2 ± 0.5 Gyr (Padova) and 10.5 ± 0.5 Gyr (Dartmouth). The cluster ridge line is best approximated by the α-enhanced Dartmouth isochrones. Placing our relative ages on an absolute age scale, we find ages of 10.9 ± 0.5 Gyr (from the magnitude difference between the main-sequence turn-off and the horizontal branch) and 11.5 ± 0.5 Gyr (from the absolute magnitude of the horizontal branch), respectively. These five different age determinations are all lower by $2 - 3$ Gyr than the ages of the oldest Galactic globular clusters of comparable metallicity. Therefore we confirm the earlier finding that the oldest globular cluster in the Small Magellanic Cloud, NGC 121, is a few Gyr younger than its oldest counterparts in the Milky Way and in other nearby dwarf galaxies such as the Large Magellanic Cloud, Fornax, and Sagittarius. If it were accreted into the Galactic halo, NGC 121 would resemble the "young halo globulars", although it is not as young as the youngest globular clusters associated with the Sagittarius dwarf. The young age of NGC 121 could result from delayed cluster formation in the Small Magellanic Cloud or result from the random survival of only one example of an initially small number star clusters.

Subject headings: star clusters: ages — star clusters: individual (NGC 121) — galaxies: Magellanic Clouds — galaxies: stellar content — stars: horizontal branch — stars: late-type

1. INTRODUCTION

Characterizing old stellar populations provide important constraints on the early star formation histories of galaxies. Only the satellite galaxies of the Milky Way (MW) are sufficiently close to resolve individual stars well below the oldest main-sequence turn-offs, which is a pre-condition for accurate photometric age dating of old stellar populations. All Local Group galaxies, for which adequate data exist, appear to contain stars older than 10 Gyr (Grebel & Gallagher 2004). This result is based on main-sequence turn-off photometry of globular clusters and field populations in Galactic satellites and a few more distant Local Group galaxies (e.g., Brown et al. 2007; Cole et al. 2007), as well as the detection of horizontal branch stars (including RR Lyrae variables) in the Local Group and beyond (e.g., Held et al. 2001; Harbeck et al. 2001; Sarajedini et al. 2002; Clementini et al. 2003; Pritzl et al. 2004).

Globular clusters are preferred as the basis for old stellar population age tracers since they are usually single-age, single-metallicity objects facilitating comparative studies. Moreover, while globular cluster systems exhibit a range of ages (e.g., De Angeli et al. 2005), the oldest ones may belong to the most ancient surviving stellar systems to have completed their formation in the youthful Universe (e.g., Moore et al. 2006). In those nearby galaxies where relative age dating based on main-sequence photometry was carried out in comparison to the oldest globular clusters in the Milky Way, no age difference within the measurement accuracy was found (e.g., Grebel & Gallagher 2004; Brown et al. 2007; Cole et al. 2007, and references therein). The relative age dating of the oldest identifiable Population II objects thus indicates a common epoch of substantial early star formation in the Milky Way and its companions, although information about a putative, even older Population III remains to be uncovered in these objects.

A galaxy that may *not* share this common epoch of early star formation – at least not with respect to its globular clusters (e.g., Sarajedini et al. 1998) – is the Small Magellanic Cloud (SMC)[8]. The SMC is one of the

---

[*] Based on observations made with the NASA/ESA Hubble Space Telescope, obtained at the Space Telescope Science Institute, which is operated by the Association of Universities for Research in Astronomy, Inc., under NASA contract NAS 5-26555. These observations are associated with program GO-10396.

[1] Astronomical Institute, Department of Physics and Astronomy, University of Basel, Venusstrasse 7, CH-4102 Binningen, Switzerland

[2] Department of Astronomy, University of Wisconsin, 475 North Charter Street, Madison, WI 53706-1582

[3] Astronomisches Rechen-Institut, Zentrum für Astronomie der Universität Heidelberg, Mönchhofstr. 12–14, D-69120 Heidelberg, Germany

[4] Space Telescope Science Institute, 3700 San Martin Drive, Baltimore, MD 21218

[5] INAF - Osservatorio Astronomico di Bologna, Via Ranzani 1, 40127 Bologna, Italy

[6] Department of Physics and Astronomy, University of California at Los Angeles, 430 Portola Plaza, Los Angeles, CA 90095-1547

[8] There may be additional exceptions in more distant dwarf irregular galaxies regarding the common epoch of earliest Population II star formation, although also these galaxies evidently con-

closest and therefore best studied dwarf galaxies orbiting our Galaxy.

While the SMC hosts a large number of intermediate-age and young star clusters, it only contains one "old" globular cluster, NGC 121, which is also the most massive star cluster. NGC 121 is located $\sim 2.4^\circ$($\sim$3 kpc) west of the SMC bar at ($\alpha_{J2000.0}$, $\delta_{J2000.0}$) = ($0^h26^m47.0^s$, $-71^\circ32'12.0''$).

NGC 121 is the only cluster in the SMC that is sufficiently old to have developed an extended red horizontal branch (Stryker et al. 1985) and to contain RR Lyrae stars. Indeed, whether or not to call a star cluster a globular cluster is a matter of definition. In this case we refer to Salaris & Girardi (2002) who consider Lindsay 1 as having a stumpy red clump and not a red horizontal branch. Three RR Lyrae stars were discovered in NGC 121 by Thackeray (1958). Graham (1975) found a fourth RR Lyrae variable in the cluster and an additional 75 in a 1 × 1.3 square degree field centered on NGC 121. Studies of various clusters in the LMC and in the MW showed that the presence of RR Lyrae variables indicates that the parent population is as old as or older than $\sim$ 10 Gyr.

An important question is whether NGC 121 is as old as the typical old globular clusters in the Large Magellanic Cloud (LMC) and in the MW. Previous studies found ages ranging from 8 to 14 Gyr for NGC 121 (Stryker et al. 1985; Walker 1991; Mighell et al. 1998; Udalski 1998; Shara et al. 1998; Dolphin et al. 2001) using a variety of different techniques. Studies based on the deepest available color-magnitude diagrams from Hubble Space Telescope (HST) observations with the Wide Field and Planetary Camera 2 (WFPC2) indicate an age of 10 to 10.6 Gyr for NGC 121, suggesting that this globular cluster is several Gyr younger than the oldest globulars in other nearby galaxies and in the MW (Shara et al. 1998; Dolphin et al. 2001).

The capabilities of the Advanced Camera for Surveys (ACS) provide an improvement in both sensitivity (depth) as well as angular resolution, which is essential for a reliable photometric age determination in this dense star cluster. Here we present deep photometry of NGC 121 obtained with ACS aboard the HST. We determine the age of NGC 121 utilizing both absolute and relative methods (e.g., Chaboyer et al. 1996). The current study is the first in a series of papers based on HST studies of rich intermediate-age and old star clusters in the SMC.

In addition to NGC 121, six intermediate-age SMC star clusters have been observed as part of our program: Lindsay 1, Kron 3, NGC 339, NGC 416, Lindsay 38 and NGC 419. We will derive fiducial ridgelines and fit isochrones to obtain accurate ages for each cluster using the same reduction techniques and isochrone models as described here (see § 2-4), and will present our results in future papers. In Table 1 we list the cluster identification, date of observation, passband, exposure times and location of all clusters in our HST program (GO-10396; principal investigator: J. S. Gallagher).

In the next Section we describe the data reduction procedure. In § 3 we present the color-magnitude diagram (CMD) of NGC 121 and discuss its main features. In § 4 we describe our age derivation methods and present our results.

2. OBSERVATIONS AND REDUCTIONS

The SMC cluster NGC 121 was observed with HST's ACS on 2006 March 21 as part of our program focused on star clusters and field stellar populations in the SMC. The program aims at exploring the star formation history and properties of the SMC using both a number of carefully selected clusters and field regions. For NGC 121 we obtained imaging in the F555W and F814W filters, which resemble the Johnson V and I filters in their photometric properties (Sirianni et al. 2005). The images were obtained using the Wide Field Channel (WFC) of ACS and cover an area of $200'' \times 200''$ with a pixel scale of ~ 0.05 arcsec. One set of exposures was taken at the nominal position of the cluster center. Four long exposures were obtained in each filter for hot pixel removal and to fill the gap between the two halves of the 4096 × 4096 pixel detector. Each pointing has an exposure time of 496 s in the F555W, and 474 s in the F814W filter. Moreover, two short exposures were taken in each filter with an exposure time of 10 s in F555W and 20 s in F814W.

The data set was processed adopting the standard Space Telescope Science Insitute ACS calibration pipeline (CALACS) to subtract the bias level and to apply the flat field correction. For each filter, the short and long exposures were co-added independently using the MULTIDRIZZLE package (Koekemoer et al. 2002). With this package the cosmic rays and hot pixels were removed and a correction for geometrical distortion was applied. The resulting NGC 121 data consist of one 40 s and one 1940 s exposure in F555W and one 20 s as well as one 1896 s exposure in F814W. The two short exposures allowed us to measure brighter stars that are saturated in the long exposures.

The photometric reductions were carried out using the DAOPHOT package in the IRAF environment [9]. We discarded saturated foreground stars and background galaxies using the *Source Extractor* package (Bertin & Arnouts 1996).

Due to the different crowding and signal-to-noise ratio properties of the long and the short exposure images, photometry involving point spread function (PSF) fitting was only performed on the long exposures. For the short exposures we used aperture photometry, which turned out to yield smaller formal errors than PSF photometry. We ran DAOPHOT on our data and set the detection threshold at 1 σ above the local background level in order to detect even the faintest sources. The list of stars detected in the F814W image was then used as coordinate input list to identify the stars in the F555W image and serve as our coordinate reference. 49493 sources were found to be common to both long exposure frames. For these sources, we performed aperture photometry using an aperture radius of 3 pixels. We then constructed a PSF by combining 150 bright and isolated stars that were distributed fairly uniformlly across the image. Fi-

---

tain old populations (e.g., Grebel 2001; Makarova et al. 2002)

[9] IRAF is written and supported by the IRAF programming group at the National Optical Astronomy Observatories (NOAO) in Tuscon, Arizona. NOAO is operated by the Association of Universities for Research in Astronomy, Inc. under cooperative agreement with the National Science Foundation.

TABLE 1
Journal of Observation

Cluster	Image Name	Date (yy/mm/dd)	Filter	Total Exposure Time (s)	R.A.	Dec.
NGC 121	J96106030	2006/03/21	F555W	40.0	$0^h26^m42.98^s$	$-71^\circ32'16.54''$
	J96106040			1984.0	$0^h26^m43.26^s$	$-71^\circ32'14.61''$
	J96106010		F814W	20.0	$0^h26^m42.98^s$	$-71^\circ32'16.54''$
	J96106020			1896.0	$0^h26^m43.26^s$	$-71^\circ32'14.61''$
Lindsay 1	J96105030	2005/08/21	F555W	40.0	$0^h03^m53.19^s$	$-73^\circ28'15.74''$
	J96105040			1984.0	$0^h03^m52.66^s$	$-73^\circ28'16.47''$
	J96105010		F814W	20.0	$0^h03^m53.19^s$	$-73^\circ28'15.74''$
	J96105020			1896.0	$0^h03^m52.66^s$	$-73^\circ28'16.47''$
Kron 3	J96107030	2006/01/17	F555W	40.0	$0^h24^m41.64^s$	$-72^\circ47'47.49''$
	J96107040			1984.0	$0^h24^m41.92^s$	$-72^\circ47'45.49''$
	J96107010		F814W	20.0	$0^h24^m41.64^s$	$-72^\circ47'47.49''$
	J96107020			1896.0	$0^h24^m41.92^s$	$-72^\circ47'45.49''$
NGC 339	J96104030	2005/11/28	F555W	40.0	$0^h57^m47.40^s$	$-74^\circ28'26.25''$
	J96104040			1984.0	$0^h57^m47.13^s$	$-74^\circ28'24.16''$
	J96104010		F814W	20.0	$0^h57^m47.40^s$	$-74^\circ28'26.25''$
	J96104020			1896.0	$0^h57^m47.13^s$	$-74^\circ28'24.16''$
NGC 416	J96121030	2006/03/08	F555W	40.0	$1^h07^m53.59^s$	$-72^\circ21'02.47''$
	J96121040			1984.0	$1^h07^m54.09^s$	$-72^\circ21'01.79''$
	J96121010		F814W	20.0	$1^h07^m53.59^s$	$-72^\circ21'02.47''$
	J96121020			1896.0	$1^h07^m54.09^s$	$-72^\circ21'01.79''$
Lindsay 38	J96102030	2005/08/18	F555W	40.0	$0^h48^m57.14^s$	$-69^\circ52'01.766''$
	J96102040			1940.0	$0^h48^m56.76^s$	$-69^\circ52'03.07''$
	J96102010		F814W	20.0	$0^h48^m57.14^s$	$-69^\circ52'01.76''$
	J96102020			1852.0	$0^h48^m56.76^s$	$-69^\circ52'03.07''$
NGC 419	J96103030	2006/01/05	F555W	40.0	$1^h08^m12.53^s$	$-72^\circ53'17.72''$
	J96103040			1984.0	$1^h08^m12.71^s$	$-72^\circ53'15.49''$
	J96103010		F814W	20.0	$1^h08^m12.53^s$	$-72^\circ53'17.72''$
	J96103020			1896.0	$1^h08^m12.71^s$	$-72^\circ53'15.49''$

nally, PSF photometry was carried out.

The photometric calibration was accomplished by converting the magnitudes of the individual stars to the standard ACS magnitude system by using an aperture with a radius of $0.5''$ (or 10 pixels on the image), in combination with the aperture correction from the $0.5''$ aperture radius to infinity and the synthetic zero points for the ACS/WFC (Sirianni et al. 2005). The aperture correction was derived for each frame independently. The objects found in both images were cross-identified and merged with a software package written at the Bologna Observatory by P. Montegriffo (private communication). Altogether we were able to cover a luminosity range of $\sim$ 10 magnitudes after combining the resultant photometry of the short and long exposures.

In Figure 1 we show the photometric errors assigned by DAOPHOT. For stars measured on the short exposures, the formal photometric errors remain negligible over a wide range of magnitudes. In the long exposures, all the brighter stars with $m_{555} < 19.3$ mag and $m_{814} < 19.5$ mag are saturated. At $m_{555,814} \sim$ 19.6 mag, the short exposure (*blue dots*) and aperture photometry from the long exposure (*black dots*) samples were combined, and for stars fainter than $m_{555,814} \sim$ 22.2 mag, long exposure PSF photometry (*red dots*) was used. We chose where to cut between the aperture and PSF photometry catalogues based on the m_{555} data and adopted the same value for m_{814} so as to avoid a color slope associated with this division. For our study, we rejected all stars with a σ error larger than 0.2 mag and a DAOPHOT sharpness parameter $-0.2 \leq s \leq 0.2$ in both filters. To obtain a superior CMD, we discarded all stars within a radius of $35''$ from the cluster center, which excludes the very dense core of the cluster. With this selection, our final sample contains 17464 stars common in both filters.

3. THE COLOR-MAGNITUDE DIAGRAM

The resulting color-magnitude diagram (CMD) of NGC 121 and its surroundings is shown in Figure 2. Our CMD for NGC 121 reaches $\sim$3.5 mag below the MSTO ($\sim$ 0.5 magnitudes deeper than the previous deepest available photometry), which allows us to carry out the most accurate age measurements obtained so far. The CMD shows a well-populated main sequence (MS), subgiant branch (SGB), red giant branch (RGB), horizontal branch (HB), and asymptotic giant branch (AGB). The gap on the RGB at $m_{555} \sim 20$ mag is an artificial feature due to small number statistics resulting from our exclusion of crowded stars in the cluster center. NGC 121 appears to be a single-age population object just as one would expect for a canonical star cluster. As expected, there is no obvious evidence for field star contamination by younger populations due to the location of NGC 121 in a low-density area in the outer parts of the SMC. Within the field of view of the ACS and at the high Galactic latitude of the SMC, Galactic foreground contamination is very low (e.g., Ratnatunga & Bahcall 1985).

Another possible contamination source is the massive and extended Galactic globular cluster 47 Tuc, which has a tidal radius of 42.86 arcmin (Harris 1996) and an angular distance from NGC 121 of $\sim$ 32 arcmin.

We visually estimated the location of the center of NGC 121 on the image and selected all stars within an

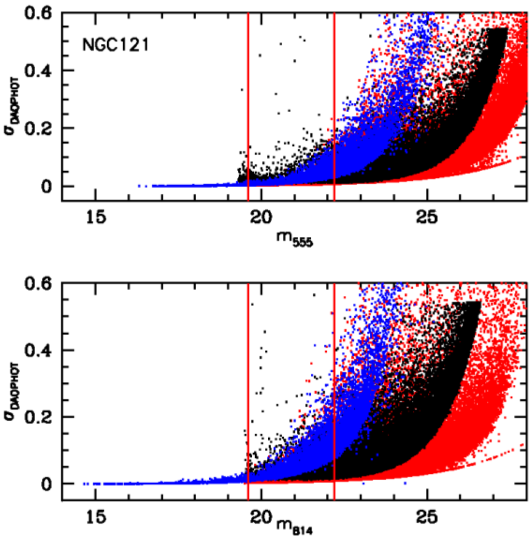

FIG. 1.— Photometric errors assigned by DAOPHOT to stars in the short exposures (blue dots), in the aperture photometry from the long (red dots), and on the PSF photometry from the long (black dots) exposures. Note the very small formal errors in the aperture photometry of the short exposures. Stars brighter than ∼ 19.3 mag in the long F555W exposure and brighter than ∼ 19.5 mag in the long F814W exposure are saturated and are therefore not shown. The lower envelope of the error distribution of the stars in the short and long F555W exposure (aperture photometry) cross over at $m_{555,814}$ = 19.6 mag, and in the aperture and PSF photometry at $m_{555,814}$ = 22.2 mag (also indicated by two thin vertical lines). Here the photometry of the short and long exposures was combined. For the F814W exposures we chose the same magnitude value in order to avoid introducing a color slope in the color-magnitude diagram of the resultant data set.

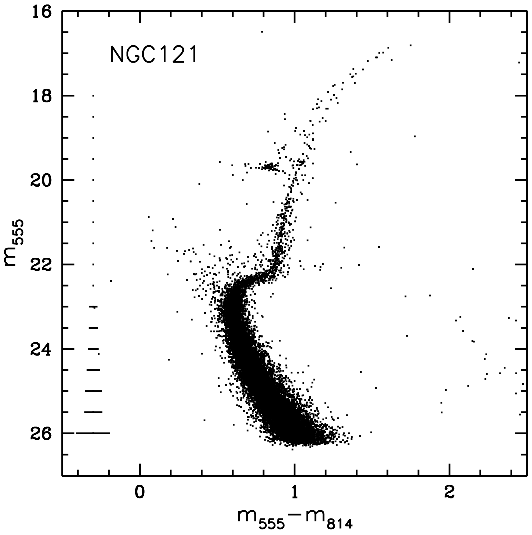

FIG. 2.— Color-magnitude diagram of NGC 121 and its surroundings. Stars within a radius of 35” from the cluster center have been discarded. All stars with ”good” photometry ($\sigma \leq 0.2$ mag and $0.2 \geq$ sharpness ≥ -0.2) are shown; 17464 stars in total. Representative errorbars (based on the errors assigned by DAOPHOT) are shown on the left for the $m_{555} - m_{814}$ color.

annulus of 35″ and 45″ to create a bona fide sample. This CMD is displayed in Figure 3. There is no evidence for a binary sequence in NGC 121, but we cannot exclude their presence, due to the photometric error. The aforementioned traces of minor field contamination have mainly vanished. Due to crowding, incompleteness be-

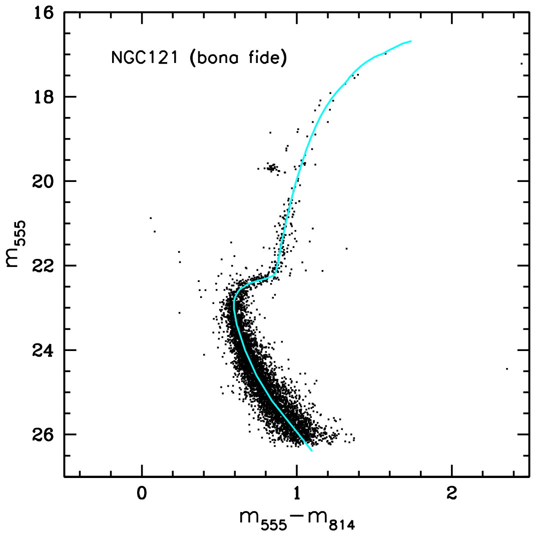

FIG. 3.— Color-magnitude diagram of all stars within an annulus between 35″ and 45″ of NGC 121. We used this CMD for the determination of a representative color-magnitude ridgeline of NGC 121 (cyan line). This CMD contains 5112 stars. Only stars with good photometry ($\sigma \leq 0.2$ mag and $0.2 \geq$ sharpness ≥ -0.2) are shown.

comes significant at the faint end of the MS: This affects particularly faint stars in the cluster center. Hence in Figure 3 the MS becomes less densely populated at fainter magnitudes.

The red HB is well populated and extends into the RR Lyrae instability strip (Clementini et al. 2007, in prep). The presence of a red HB provides a circumstantial suggestion that NGC 121 may be younger than old Galactic and LMC globular clusters, since the HBs of the oldest globular clusters tend to extend farther into the blue (e.g., Olszewski et al. 1996; Olsen et al. 1998; Mackey & Gilmore 2004). Red HBs, however, can also be due to a ”second parameter” other than age affecting the HB morphology (e.g., Lee et al. 1994; Buonanno et al. 1997; Harbeck et al. 2001; Catelan et al. 2001). Since a true HB is present, an age measurement for NGC 121 can be made using the ΔV_{TO}^{HB} age measurement, which we will do in § 4.2. This method requires the determination of the apparent mean magnitude of the HB. Our data yield $m_{555,HB}$ = 19.71 ± 0.03 mag for this observable, which is in agreement with the magnitudes determined by Shara et al. (1998), Alves & Sarajedini (1999) and Dolphin et al. (2001).

At m_{555} = 19.58 ± 0.03 mag we find the NGC 121 RGB bump ($m_{555,Bump}$) which is 0.06 mag brighter than the magnitude found by Alves & Sarajedini (1999). The difference in luminosity is due to the exclusion of the center stars. If we determine the $m_{555,Bump}$ on the entire sample, we obtain $m_{555} = 19.52 \pm 0.04$ mag, which is in excellent agreement with the magnitude found by Alves & Sarajedini (1999). This feature is predicted by stellar evolution models, which also show that the luminosity of the RGB bump is dependent on the metallicity and age of the cluster. When the metallicity is known the difference between V_{HB} and V_{Bump} can be used as an age indicator.

Above the MS turn-off, Shara et al. (1998) found 42 candidate blue straggler stars (BSS). Evolved descen-

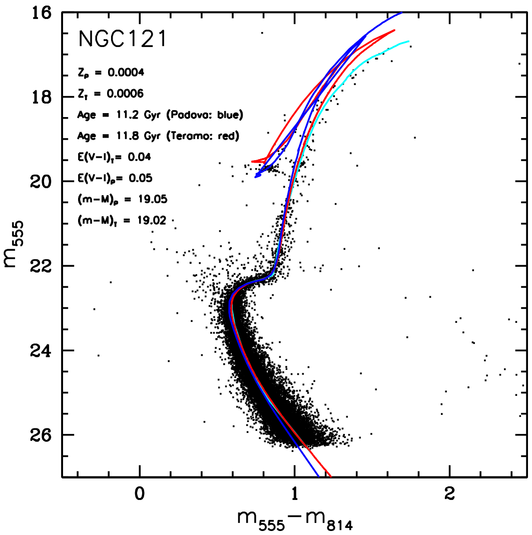

Fig. 4.— The CMD of NGC 121 with the best-fitting isochrones of two different models: The blue solid line shows the best-fitting Padova (Girardi, "private communication", Girardi et al. 2000) isochrone that is closest to the spectroscopically measured metallicity of the cluster. The red solid line is the best-fitting Teramo (Pietrinferni et al. 2004) isochrone approximating the known metallicity. Neither model is α-enhanced. The cyan solid line is our fiducial ridgeline. The fitting parameters are listed in the plot legend.

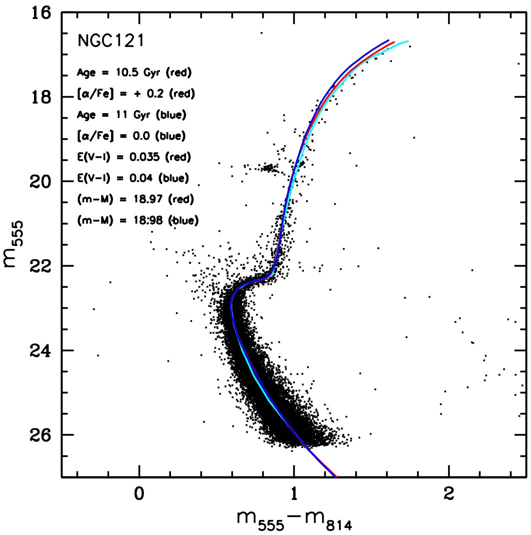

Fig. 5.— The NGC 121 CMD with the best-fitting Dartmouth (Dotter et al. 2007) isochrones overplotted in red. As before, the cyan line represents our fiducial for NGC 121. The fit parameters are listed in the plot. Note the excellent agreement of this α-enhanced isochrone with the observed CMD.

dants of the BSSs are important as possible sources of stars lying above the traditional HB (e.g., Catelan 2005). In our ACS study we recovered the Shara et al. (1998) BSS sample and also found more stars in the BSS region of which some (about 20) turned out to be pulsating variables (dwarf Cepheids). These stars will be discussed in Clementini et al. (2007, in preparation) where we will present the results of an HST study of variable stars in NGC 121.

4. AGE OF NGC 121

4.1. *Age Based on Isochrone Fits*

Age determinations of star clusters using isochrones depend crucially on the interstellar extinction, distance, and metallicity of the cluster, as well as on the chosen isochrone models. In fitting isochrones to the CMD of NGC 121 we adopted the spectroscopic metallicity measurement of [Fe/H] = -1.46 ± 0.10 from Da Costa & Hatzidimitriou (1998, see also Johnson et al. 2004) on the metallicity scale introduced by Zinn & West (1984) (ZW84). The distance and the extinction were treated as free parameters. The SMC distance modulus is $(m-M)_0$ = 18.88 ± 0.1 mag (60 kpc) (e.g., Storm et al. 2004), but due to the large depth extension of the SMC along the line of sight we adjusted the distance modulus $(m-M)_0$ to produce the best isochrone fits to our CMD data.

For easier comparison to the isochrones, we first derived a fiducial ridgeline (Table 2), which reproduces the mean location of the stellar distribution in the CMD (exempting the HB). In order to determine the ridgeline, we separated the cluster center CMD into three sections: the MS, the SGB and the RGB. On the MS we determined the mode of the color distribution in magnitude bins of 0.3 mag width. For the SGB, we performed a linear least squares fit of a polynomial of 5th order to a Hess diagram of this region in the CMD. Finally, the RGB was fit by a third-order polynomial of the mean color, again in magnitude bins with a size of 0.3 mag each. The resulting ridgeline is shown in Fig. 3 as a cyan line.

We fitted our m_{555} vs. m_{555}-m_{814} CMD with three different isochrone models: Padova isochrones (Girardi, "private communication", Girardi et al. 2000) [10], Teramo isochrones (Pietrinferni et al. 2004), both with scaled solar isochrones ([α/Fe] = 0.0), and Dartmouth isochrones (Dotter et al. 2007) with both [α/Fe] = 0.0 and +0.2. The Padova isochrone grid has an age resolution of log(t)=0.05, the Teramo isochrone grid of 0.1 Myr and the Dartmouth isochrone grid of 0.5 Gyr. Our adopted spectroscopic metallicity of [Fe/H] = -1.46 corresponds most closely to Z = 0.0004 in the Padova models, to Z = 0.0006 in the Teramo models, and to [Fe/H] = -1.49 in the Dartmouth models. All three sets of isochrone models are available in the standard ACS color system.

We fitted a large number of isochrones using different combinations of reddening, age, and distance. For each set of models, we selected the isochrone that best matched the observed data (Fig. 4, Fig. 5).

First we discuss Figure 4. Our best-fit age using Padova isochrones is 11.2 Gyr with $(m-M)_0$ = 19.05 mag and E_{V-I} = 0.05. The best fitting Teramo isochrone yields an age of t = 11.8 Gyr, $(m-M)_0$ = 19.02 mag, and E_{V-I} = 0.04. On the MS, both the Teramo isochrone and the Padova isochrones trace the ridge line almost perfectly. At the faint end of the MS, the Padova isochrone continues further to the blue than the Teramo isochrone and our derived ridge line; however, this only becomes more apparent at magnitudes of $m_{555} \sim 25.5$ mag and below. Both isochones also provide an excellent approximation to the SGB and to the lower RGB up to about half a magnitude below the HB.

At brighter magnitudes, the two isochrones deviate increasingly to the blue of the observed upper RGB. Here the Padova isochrone shows the strongest difference, deviating by approximately 0.38 mag in color from the observed tip of the RGB. The isochrone shows a magnitude for the base of the red HB that is about 0.5 mag fainter than the observed one. Unlike Teramo and Dartmouth, the Padova isochrone also models the AGB and its tip, which is ~ 1 mag brighter than the tip of the RGB. The Teramo isochrone is too blue by about 0.23 mag at the magnitude of the tip of the RGB and indicates a magnitude for the base of the red HB that is 0.2 mag too bright.

---

[10] http://pleiadi.pd.astro.it/isoc_photsys.02/isoc_acs_wfc/index.html

If we had no prior knowledge of the metallicity of NGC 121 and were to use the upper RGB as a metallicity indicator, a better fit would be obtained by choosing isochrones of a different metallicity or α abundance. The problems of various isochrone models of given metallicities in reproducing the upper red giant branches of globular clusters with the same metallicities are a well-known problem (e.g., Grebel 1997, 1999). Our Figure 4 reflect the general failure of the chosen stellar evolutionary models to simultaneously reproduce the major features of CMDs (Gallart et al. 2005) in spite of the excellent fit to the lower RGB, SGB, and MS. Fortunately the latter are the most age-sensitive features of the CMD.

The isochrone model provided by Dotter et al. (2007) with $[\alpha/\mathrm{Fe}] = +0.2$ yield the best fit to the CMD (Fig. 5). The best-fit isochrone has the parameters $t = 10.5$ Gyr, $(m - M)_0 = 18.96$ mag, and $E_{V-I} = 0.035$, using the α-enhanced isochrones of $[\alpha/\mathrm{Fe}] = +0.2$. *All* the major features of the CMD are very well reproduced, including the upper RGB where the isochrone is offset slightly to the blue relative to the fiducial ridgeline. This offset is no more than 0.01 to 0.02 on average along the entire upper RGB; i.e., even the *slope* of the RGB is very well reproduced along its entire extent. Unfortunately the stellar evolution models used here terminate at the He flash, and therefore do not fit the HB or the AGB.

Is our use of α-enhanced models justified? For NGC 121 a value of $[\mathrm{Ca/Fe}] = +0.24$ has been measured, which is similar to the outer LMC cluster Hodge 11 and to the old Galactic outer halo clusters with $[\mathrm{Ca/Fe}] = +0.3$ (Johnson et al. 2004). Consequently, we assume that NGC 121 also is enhanced in α-elements. We note that in this respect NGC 121 differs from the general trend observed in red giant stars in the LMC and in dwarf spheroidal galaxies, where the $[\alpha/\mathrm{Fe}]$ ratios at a given [Fe/H] tend to be lower by up to a few tenths of a dex than in the Galactic halo (e.g., Hill et al. 2000; Shetrone et al. 2001; Fulbright 2002; Pritzl et al. 2005; Johnson et al. 2006; Koch et al. 2007).

When we adopt the values for distance and reddening, but fit the cluster with an isochrone scaled solar, NGC 121 gets a slightly older age of 11 Gyr. The isochrone model with $[\alpha/\mathrm{Fe}] = 0.0$ still provides a better fit than the Teramo or Padova models, but has an offset of ~ 0.05 on average along the upper RGB. Past studies found that α-enhanced models imply a higher luminosity and temperature for the same mass than the solar scaled models and therefore an older age for the same magnitude (e.g., VandenBerg et al. 2000). The Dartmouth models show exactly the opposite behavior. This is because in these models an increase in $[\alpha/\mathrm{Fe}]$ is accompanied by a corresponding increase of the total metallicity Z, which makes the isochrones cooler at constant age and [Fe/H].

Finally, we note that the derived reddenings agree with the extinction $A_V = 0.1 \pm 0.03$ from the Schlegel et al. (1998) maps. The reddening law of O'Donnell (1994) is assumed.

In the Figures 6 and 7 we show a range of isochrones for the three sets of stellar evolution models in order to illustrate the age uncertainty in a given model. The finally chosen, "best" isochrone is always displayed along with two younger and two older isochrones. For the cases of the Teramo and Padova models, the two isochrones that are one age step younger or older than the chosen, central isochrone provide an upper or lower envelope for the location of the high-density part of the SGB, the MS turn-off, and the base of the RGB. For the Dartmouth isochrones the outermost isochrones provide this envelope. Considering the high quality of the fit of the central isochrone in this CMD region in all models and the larger deviations of the adjacent isochrones, we estimate that the resultant age uncertainty is of the order of approximately ±0.5 Gyr for the Teramo and Dartmouth isochrones and ±0.7 Gyr for the Padova isochrones.

4.2. *Empirical Age Estimates*

4.2.1. *Vertical Method*

To check the reliability of the isochrone ages, we use a reddening-independent method to derive relative ages of NGC 121. This method is also independent of the photometric zeropoint of our data. This "vertical method" relies on the fact that the absolute magnitude of the MSTO depends on the age of the cluster (e.g., Alves & Sarajedini 1999), while the absolute magnitude of the HB remains approximately age-independent for clusters older than $t \gtrsim 10$ Gyr (e.g., Girardi & Salaris 2001). We measure the apparent magnitudes of the MSTO and HB, i.e., V_{TO} and V_{HB}, in order to obtain the magnitude difference ΔV^{HB}_{TO}. With increasing age, a cluster has generally larger values of this parameter since the MS moves to fainter magnitudes. Unfortunately, the determination of these two points comes with significant uncertainties. ΔV^{HB}_{TO} is hard to measure accurately both because of the width of the HB in luminosity and the MSTO's vertical extent in the turn-off region.

First, we calculate the magnitude difference $\Delta m^{HB}_{TO,555}$ between the HB and the MSTO, as originally described by Iben & Faulkner (1968). Because m_{555} is proportional to V and we are only interested in the magnitude difference, which we measure at constant color, there is no need to transform the magnitudes from the ACS system to V and I magnitudes (Sirianni et al. 2005). We follow the general definition of the MSTO as the bluest point along the MS; in our case represented by the bluest point on the ridgeline. We find the MSTO at $m_{TO,555} = 22.98 \pm 0.05$ mag, $(m_{555} - m_{814}) = 0.59 \pm 0.005$ mag. As described in Section 3, the mean HB magnitude is $m_{HB,555} = 19.71 \pm 0.03$ mag. This yields a $\Delta m^{HB}_{TO,555} = 3.27 \pm 0.06$ mag. Our result is only slightly lower than former values, e.g., $\Delta V^{HB}_{TO} = 3.32$ determined by Stryker et al. (1985), 3.33 by Shara et al. (1998) or 3.29 by Dolphin et al. (2001). Buonanno et al. (1989) published a mean value of $\Delta V^{HB}_{TO} = 3.55$ mag for old Galactic halo globular clusters (GC). The $\Delta m^{HB}_{TO,555}$

TABLE 2
Ridgeline of NGC 121

$m_{555} - m_{814}$	m_{555}	$m_{555} - m_{814}$ cont.	m_{555} cont.
1.7400	16.6859	1.0000	19.9538
1.7300	16.6916	0.9900	20.0855
1.7200	16.7011	0.9800	20.2218
1.7100	16.7107	0.9700	20.3630
1.7000	16.7224	0.9600	20.5090
1.6900	16.7339	0.9500	20.6601
1.6800	16.7483	0.9400	20.8162
1.6700	16.7605	0.9300	20.9774
1.6600	16.7834	0.9200	21.1440
1.6500	16.8001	0.9100	21.3159
1.6400	16.8177	0.9000	21.4932
1.6300	16.8381	0.8900	21.6762
1.6200	16.8554	0.8800	21.8899
1.6100	16.8706	0.8700	22.0599
1.6000	16.8867	0.8600	22.1921
1.5900	16.9098	0.8600	22.1933
1.5800	16.9289	0.8500	22.2305
1.5700	16.9540	0.8400	22.2520
1.5600	16.9712	0.8300	22.2660
1.5500	16.9874	0.8200	22.2770
1.5400	17.0008	0.8100	22.2890
1.5300	17.0153	0.8000	22.3050
1.5200	17.0309	0.7900	22.3180
1.5100	17.0477	0.7800	22.3280
1.5000	17.0658	0.7700	22.3380
1.4900	17.0851	0.7600	22.3480
1.4800	17.1057	0.7500	22.3570
1.4700	17.1276	0.7400	22.3670
1.4600	17.1508	0.7300	22.3770
1.4500	17.1753	0.7200	22.3880
1.4400	17.2013	0.7100	22.4010
1.4300	17.2286	0.7000	22.4120
1.4200	17.2575	0.6900	22.4260
1.4100	17.2877	0.6800	22.4520
1.4000	17.3195	0.6700	22.4710
1.3900	17.3528	0.6600	22.5020
1.3800	17.3877	0.6500	22.5190
1.3700	17.4241	0.6400	22.5410
1.3600	17.4621	0.6300	22.5720
1.3500	17.5018	0.6200	22.6240
1.3400	17.5432	0.6100	22.6890
1.3300	17.5962	0.6000	22.7610
1.3200	17.6378	0.5950	22.8500
1.3100	17.6904	0.5950	23.0310
1.3000	17.7246	0.6125	23.4000
1.2900	17.7605	0.6670	24.0000
1.2800	17.7983	0.7400	24.6000
1.2700	17.8379	0.8400	25.2000
1.2600	17.8794	0.9700	25.8000
1.2500	17.9231	1.1000	26.4000
1.2400	17.9690		
1.2300	18.0171		
1.2200	18.0676		
1.2100	18.1205		
1.2000	18.1761		
1.1900	18.2343		
1.1800	18.2952		
1.1700	18.3590		
1.1600	18.4257		
1.1500	18.4955		
1.1400	18.5685		
1.1300	18.6447		
1.1200	18.7242		
1.1100	18.8071		
1.1000	18.8936		
1.0900	18.9837		
1.0800	19.0775		
1.0700	19.1752		
1.0600	19.2767		
1.0500	19.3823		
1.0400	19.4920		
1.0300	19.6059		
1.0200	19.7241		
1.0100	19.8367		

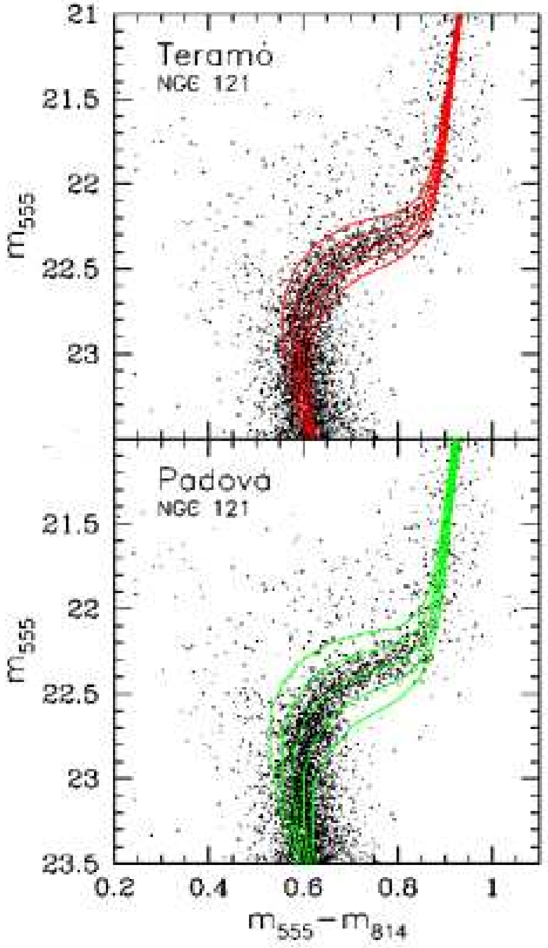

Fig. 6.— The color-magnitude diagram of NGC 121 after zooming in on the region of the main-sequence turn-off, subgiant branch, and lower red giant branch. In the upper panel, we show Teramo isochrones as solid lines, covering an age range of 10, 10.9, 11.8, 12.6, and 13.5 Gyr. These are the age steps in which these isochrones are provided (Pietrinferni et al. 2004). The central isochrone is our chosen best-fitting isochrone. In the lower panel we show the same plot for Padova isochrones (solid lines) in the Padova age steps of 8.9, 10, 11.2, 12.6, and 14 Gyr (Girardi, "private communication", Girardi et al. 2000). All other parameters are the same as in Figs. 4 and 5.

of NGC 121 is 0.28 mag smaller than this value, which indicates that NGC 121 is younger than most of the older *Galactic* GCs.

Walker (1992) (see also Buonanno et al. 1989) found a relation between age and ΔV_{TO}^{HB} based on a study of 41 Galactic globular clusters. Adopting again a metallicity of [Fe/H] $= -1.46 \pm 0.10$, we find with the formula $\log t = -0.045[\mathrm{Fe/H}] + 0.37 \Delta V_{TO}^{HB} - 0.24$ an age of 10.9±0.5 Gyr for NGC 121.

4.2.2. *Age Estimate using $M_V(HB)$*

In order to compare our data directly with Dolphin et al. (2001), we use the age calibration provided by Chaboyer et al. (1996b) as was done by these authors. For this purpose we must adopt the metallicity Fe/H] $= -1.19 \pm 0.12$ of Da Costa & Hatzidimitriou (1998) on the metallicity scale introduced by Carretta & Gratton (1997) (CG97) to be consistent with Dolphin et al. (2001)'s calculation. Note that elsewhere in the paper we are using metallicities on the ZW84 scale which

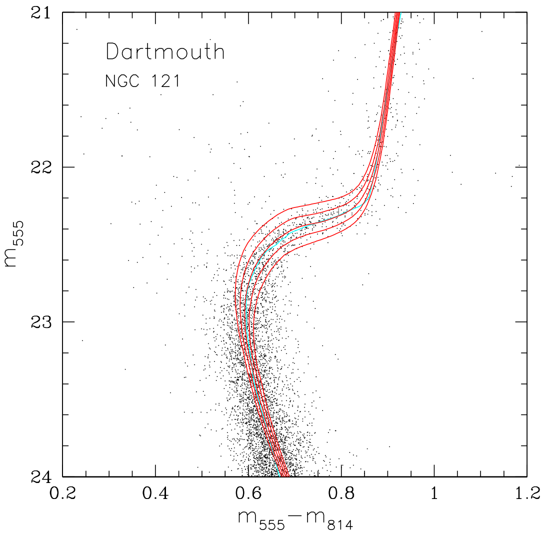

FIG. 7.— Same as Fig. 6, but for the α-enhanced Dartmouth isochrones covering an age range of 9.5, 10, 10.5, 11, and 11.5 Gyr (Dotter et al. 2007).

agrees reasonably well with the spectroscopically derived chemical abundances (Johnson et al. 2004). Using this method and the higher metallicity we determine an age of 9.7 ± 1.0 Gyr for NGC 121, which is similar to the age that Dolphin et al. (2001) found. We have to emphasize that this age is younger than the absolute ages determined in Section 4.1 due to the different metallicity scale. If we use our preferred ZW84 metallicity scale with this method we obtain an older age of 10.8 ± 1.0 Gyr.

While the measurement of V_{TO} is affected by significant observational errors (~ 0.05 mag), the color of the MSTO is well-defined. Chaboyer et al. (1996a) found that the usage of a point on the SBG brighter than the MSTO and 0.05 mag redder (V_{BTO}) provides more precise relative ages than V_{TO}. Chaboyer et al. (1996a) provide a conversion between $M_V(BTO)$ and V, I data for a grid of five metallicities. We choose the conversion for [Fe/H] $= -1.5$ because it is closest to the metallicity of NGC 121. In our data, we measured $m_{BTO,555} = 22.45 \pm 0.02$ at $(m_{555} - m_{814})_{BTO} = 0.64 \pm 0.005$ mag. To convert $m_{BTO,555}$ to the absolute magnitude $M_{BTO,555}$ we use the distance modulus derived above. This yields $M_{BTO,555} = 3.49 \pm 0.1$ mag. With the modified calibration by Johnson et al. (1999) we obtain an age of 11.50 ± 0.5 Gyr for NGC 121. We have summarized all our age results in Table 3.

4.2.3. *Red Bump*

Calculating $\Delta m^{HB}_{555,Bump} = m_{555,Bump} - m_{555,HB}$ we find -0.13 ± 0.05 mag. There is a general trend of increasing RGB bump brightness with decreasing age (Alves & Sarajedini 1999), assuming that a different "second parameter" is not affecting the position of the RGB bump. Alves & Sarajedini (1999) presented a V^{HB}_{Bump} vs. [Fe/H] diagram (their Fig. 6), where the brightness difference between the RGB bump and the HB is plotted against the cluster metallicity. If we assume that the HB magnitude does not critically depend on age, then NGC 121 is slightly older than 10 Gyr based on this relation.

TABLE 3
AGES FOR NGC 121 DERIVED IN THIS PAPER

Age [Gyr]	Method	Reference for method
10.9 ± 0.5	ΔV^{HB}_{TO}	Walker (1992) (ZW)
11.5 ± 0.5	$M_V(BTO)$	Chaboyer et al. (1996a)
10.8 ± 1.0	$M_V(HB)$	Chaboyer et al. (1996b)
11.8 ± 0.5	Isochrones	Pietrinferni et al. (2004)
11.2 ± 0.7	Isochrones	Girardi, "private communication", Girardi et al. (2000)
10.5 ± 0.5	Isochrones	Dotter et al. (2007)

[a] All derived ages are listed along with the method applied. In all cases, we adopted the ZW84 metallicity scale.

These comparative results are sensitive to the abundance of α-elements in NGC 121 as compared to Galactic globular clusters. Many nearby Galactic globular clusters are enhanced in α-elements relative to the solar value (Johnson et al. 2004). As mentioned earlier, spectroscopic results for NGC 121 indicate that this cluster is similarly enhanced in α elements, which means that the relative ages should not be affected as long as we confine ourselves to the comparison of globular clusters with similar α-element ratios. The fact that NGC 121 does not follow the trend of reduced [α/Fe] ratios observed in other nearby dwarf galaxies facilitates both our relative age determinations.

4.2.4. *Relative Age of NGC 121*

In Table 4 we compare the relative age of NGC 121 with those for a sample of Galactic globular clusters. While this comparison sample is located in the Galactic halo, some objects may have formed outside the Galaxy and might have been subsequently captured or accreted. We list the clusters by their identification in column (1). The [Fe/H] values are given in column (2) in the scale by Zinn & West (1984). Column (3) shows the ΔV^{HB}_{TO} and column (4) the ages obtained by using the Walker (1992) calibration. Finally, column (5) gives the relative age difference of these clusters to NGC 121 $\delta(t)_W$. For ΔV^{HB}_{TO} we adopted the values from De Angeli et al. (2005), unless differently stated (see footnotes of Table 4).

The clusters are listed in order of increasing ΔV^{HB}_{TO} and are divided into two groups. The first group shows nine "pure" GCs with similar metallicities as NGC 121. Among these nine clusters is NGC 2808 for which multiple MSTOs have been found (Piotto et al. 2007). Its ΔV^{HB}_{TO} value, derived prior to the study by (Piotto et al. 2007), is comparatively small. Even though those nine clusters have all similar metallicities, the spread in ΔV^{HB}_{TO} and therefore in age is quite large: NGC 1262 shows the lowest $\Delta V^{HB}_{TO} = 3.24$ and is similar in age to NGC 121, while NGC 6656 has $\Delta V^{HB}_{TO} = 3.55$, which makes it ~3 Gyr older than NGC 121.

The second group includes a subset of Galactic halo clusters that appear to be significantly younger than the average of the Galactic globular cluster population (e.g., Rosenberg et al. 1999; VandenBerg 2000; Salaris & Weiss 2002). Some members of this group are listed in the last part of Table 4. NGC 362 and NGC 288 are known to be a second parameter cluster pair of different ages, as reflected in their different ΔV^{HB}_{TO} (e.g., Fusi Pecci et al. 1996; Catelan et al. 2001; Bellazzini et al. 2001). As NGC 362 has a similar ΔV_{TO}^{HB} and [Fe/H] as NGC 121, it should therefore be of a similarly young age. Other members of this group of young halo globulars are IC 4499 (Ferraro et al. 1995), Ruprecht 106 (assumed to be 3–5 Gyr younger than the bulk of the Galactic globulars with similar metallicities; Da Costa et al. 1992; Buonanno et al. 1993), Arp 2 (Buonanno et al. 1995a), Terzan 7 (Buonanno et al. 1995b), and Pal 14 (Sarajedini 1997).

Among the theories that try to explain the existence of these young objects is the model according to which they are intergalactic clusters captured by the MW (Buonanno et al. 1995b), or clusters formed during interactions between the MW and the Magellanic Clouds assuming that they are on bound orbits (Fusi Pecci et al. 1995). Zinn (1993) argued that the apparent young halo globular clusters formed in dwarf galaxies that later merged with the MW. Hence the Galactic globular clusters are assumed to be a mixture of objects that formed with the MW itself (old halo group) and others accreted from destroyed dwarf satellites (young halo clusters) (see also Mackey & Gilmore 2004). At least six globular clusters are believed to be associated with the Sagittarius dwarf galaxy (e.g., Carraro et al. 2007, and references therein), providing support for the accretion scenario. Note, however, that Sagittarius is contributing both old (M54, Ter 8, Arp 2) and "young" (Ter 7, Pal 12, Whiting 1) globular clusters to the MW. Similarly, the only other Galactic dSph galaxy known to contain globular clusters, Fornax, would contribute both kinds of globulars (Buonanno et al. 1998, 1999) if it were to merge with our Galaxy. This also holds for the LMC (Olsen et al. 1998, see also discussion in Grebel, Gallagher, & Harbeck 2003).

If we take all the ages determined in this paper into account, we find that NGC 121 is consistently 2–3 Gyr younger than the oldest Galactic globular clusters (absolute age $\sim$ 13 Gyr according to Krauss & Chaboyer 2003) and LMC globular clusters. The age offset remains when comparing NGC 121 to old Galactic globular clusters in the same metallicity range (see Tab. 4, upper panel). We also show that NGC 121 is not as young as the youngest Galactic and Sagittarius globular clusters, some of which are $\sim$ 2 Gyr younger than NGC 121.

5. SUMMARY AND DISCUSSION

We derived ages for the old SMC globular cluster NGC 121 based on our high dynamic range HST/ACS photometry that extends at least three magnitudes below its MSTO. In order to obtain absolute ages, we applied three different isochrone models. These isochrone models yielded ages of 11.2 ± 0.7 Gyr (Padova), 11.8 ± 0.5 Gyr (Teramo), and 10.5 ± 0.5 Gyr (Dartmouth). We find the α-enhanced Dartmouth isochrones provide the closest approximation to the MS, SGB, and RGB, whereas the other models cannot reproduce the slope of the upper RGB. High-resolution spectroscopy indicates that NGC 121 is indeed α-enhanced (Johnson et al. 2004), a property that it shares with many of the old outer Galactic halo globulars. Given the proximity of NGC 121 to the SMC on the sky and its distance, its physical association with the SMC seems well-established.

Our determinations of relative ages for NGC 121 are consistent with the results of our absolute age determination. Relative age estimates, when converted to an absolute age scale, are 10.9 ± 0.5 Gyr (ΔV_{TO}^{HB}), 10.8 ± 1.0 ($M_V(HB)$) and 11.5 ± 0.5 Gyr ($M_{V(BTO)}$). These numbers agree well with the absolute age derivations. Our results confirm that NGC 121 is 2–3 Gyr younger than the oldest MW and LMC clusters (as also found in earlier WFPC2 studies).

NGC 121 is similar in age to the youngest globular cluster in the Fornax dSph (Buonanno et al. 1999), and to several of the young Galactic halo clusters. On the other hand, NGC 121 is not as young as some of the Sgr dwarf galaxy's globular clusters or the youngest Galactic globular clusters.

It is intriguing that the SMC – in contrast to other Galactic companion dwarf galaxies with globulars – does not contain any old classical globular clusters. But given the existence of only one cluster and the question of star cluster survival, this could be a result of the one survivor from the SMC's epoch of globular cluster formation randomly sampling an initial distribution of star cluster ages. On the other hand, in low-mass galaxies without bulges, spiral density waves, and shear it is much more difficult to destroy globular clusters through external effects. That this cluster is both younger than the Galactic mean and enhanced in α-elements may have interesting implications for the early development of the SMC.

It also is intriguing that the only globular cluster in the SMC is not very metal-poor. The SMC must have experienced substantial enrichment prior to the formation of NGC 121. In the LMC, where two main epochs of the formation of populous compact star clusters have been found (e.g., Bertelli et al. 1992), a few globular clusters are found that are old enough to exhibit blue HBs. Interestingly, these globular clusters, which are similarly old as the oldest Galactic globulars (Olsen et al. 1998), have a similar metallicity to NGC 121 (Johnson et al. 2004) (e.g., NGC 1898, NGC 2019), indicating very early chemical enrichment. The MW also contains old classical globular clusters (with blue HBs) that have similarly high metallicities as the somewhat younger NGC 121. Evidently, the conditions for and the efficiency of star formation varied in these three galaxies at early epochs.

After NGC 121 formed there was a hiatus in surviving stars clusters and thus possibly in cluster formation activity in the SMC: The second oldest SMC cluster is Lindsay 1 with an age of $\sim$ 8 Gyr (Glatt et al. 2007, in preparation). Since then compact populous star clusters formed fairly continuously until the present day in the SMC (e.g., Da Costa 2002) – in contrast to both the LMC and the MW. In forthcoming papers on our ACS photometry of SMC clusters and field populations we will explore the evolutionary history of the SMC in more detail. Clearly, clues about the early star formation history of the SMC will have to come from its old field populations.

We thank the anonymous referee for extremely useful suggestions to improve our paper. We gratefully acknowledge support by the Swiss National Science Foundation through grant number 200020-105260 and 200020-113697. Support for program GO-10396 was provided by NASA through a grant from the Space Telescope Science Institute, which is operated by the Association of Uni-

TABLE 4
Comparison of globular clusters ages (vertical method)

Cluster	$[Fe/H]_{ZW84}$	ΔV_{TO}^{HB}	Age [Gyr]	$\delta(t)_W$
NGC 121	-1.46	3.27	10.9	0
NGC 1261	-1.32	3.24	10.4	-0.5
NGC 5272	-1.66	3.24	10.8	0.1
NGC 2808	-1.36	3.25	10.6	-0.3
NGC 3201	-1.53	3.28	11.0	0.1
NGC 5904	-1.38	3.34	11.4	0.5
NGC 6254	-1.55	3.37	11.9	1.0
NGC 6218	-1.40	3.48	12.9	2.0
NGC 6752	-1.54	3.53	13.7	2.8
NGC 6656	-1.41	3.55	13.7	2.8
Pal 12	-0.94	3.17	9.45	-1.3
IG 4499	-1.75	3.25	11	0.1
NGC 362	-1.33	3.27	10.7	-0.2
Pal 14	-1.65	3.33	11.7	0.8
NGC 288	-1.40	3.45	12.6	1.7

[a] Ages were determined using the Walker (1992) calibration. The metallicity of NGC 121 was adopted from Da Costa & Hatzidimitriou (1998). The other results for NGC 121 were derived in this Paper. The data for NGC 6656 where taken from Rosenberg et al. (1999); for IGC 4499 from Ferraro et al. (1995); for Pal 12 from Rutledge et al. (1997) and for Pal 14 from Ferraro et al. (1995) and Ferraro et al. (1995); Sarajedini (1997). All other values were taken from De Angeli et al. (2005).

versities for Research in Astronomy, Inc., under NASA contract NAS 5-26555. We warmly thank Paolo Montegriffo to provide his software and Leo Girardi for the Padova isochrones in the standard ACS color system. Gisella Clementini and Monica Tosi have been partially supported by PRIN-MIUR-2004 and PRIN-INAF-2005, and Jay Gallagher also obtained helpful additional support from the University of Wisconsin Graduate School.

REFERENCES

Alves, D. R., & Sarajedini, A. 1999, ApJ, 511, 225

Bellazzini, M., Fusi Pecci, F., Ferraro, F. R., Galleti, S., Catelan, M., & Landsman, W. B. 2001, AJ, 122, 2569

Bertelli, G., Mateo, M., Chiosi, C., & Bressan, A. 1992, ApJ, 388, 400

Bertin, E., & Arnouts, S. 1996, A&AS, 117, 393

Brown, T. M., et al. 2007, ApJ, 658, L95

Buonanno, R., Corsi, C. E. & Fusi Pecci, F. 1989, A&A, 216, 80

Buonanno, R., Corsi, C. E., Fusi Pecci, F., Richer, H. B., & Fahlman,G. G. 1993, AJ, 105, 184

Buonanno, R., Corsi, C. E., Pulone, L., Fusi Pecci, F., Richer, H. B., & Fahlman,G. G. 1995b, AJ, 109, 663

Buonanno, R., Corsi, C. E., Fusi Pecci, F., Richer, H. B., & Fahlman,G. G. 1995a, AJ, 109, 650

Buonanno, R., Corsi, C., Bellazzini, M., Ferraro, F. R., & Fusi Pecci, F. 1997, AJ, 113, 706

Buonanno, R., Corsi, C. E., Zinn, R., Fusi Pecci, F., Hardy, E., & Suntzeff, N. B. 1998, ApJ, 501, L33

Buonanno, R., Corsi, C. E., Castellani, M., Marconi, G., Fusi Pecci, F., & Zinn, R. 1999, AJ, 118, 1671

Carraro, G., Zinn, R., & Moni Bidin, C. 2007, A&A, 466, 181

Carretta, E., & Gratton, R. G. 1997, A&AS, 121, 95

Catelan, M., Ferraro, F. R., & Rood, R. T. 2001a, ApJ, 560, 970

Catelan, M., Bellazzini, M., Landsman, W. B., Ferraro, F. R., Fusi Pecci, F., & Galleti, S. 2001b, AJ, 122, 3171

Catelan, M. 2005, ArXiv Astrophysics e-prints, arXiv:astro-ph/0507464

Chaboyer, B., Demarque, P., Kernan, P. J. & Krauss, L. M. 1996, Science, 271, 957

Chaboyer, B., Demarque, P., Kernan, P. J., Krauss, L. M., & Sarajedini, A. 1996a, MNRAS, 283, 683

Chaboyer, B., Demarque, P., & Sarajedini, A. 1996b, ApJ, 459, 558

Clementini, G., Held, E. V., Baldacci, L., & Rizzi, L. 2003, ApJ, 588, L85

Cole, A. A., et al. 2007, ApJ, 659, L17

Da Costa, G. S., Armandroff, T. E. & Norris, J. E. 1992, AJ, 104, 154

Da Costa, G. S. & Hatzidimitriou, D. 1998, AJ, 115, 1934

De Angeli, F., Piotto, G., Cassisi, S., Busso, G., Recio-Blanco, A., Salaris, M., Aparicio, A., & Rosenberg, A. 2005, AJ, 130, 116

Dolphin, A. E., Walker, A. R., Hodge, P. W., Mateo, M., Olszewski, E. W., Schommer, R. A., & Suntzeff, N. B. 2001, ApJ, 562, 303

Dotter, A., Chaboyer, B., Jevremović, D., Baron, E., Ferguson, J. W., Sarajedini, A., & Anderson, J. 2007, AJ, 134, 376

Ferraro, I., Ferraro, F. R., Fusi Pecci, F., Corsi, C. E. & Buonanno, R. 1995, MNRAS, 275, 1057

Fulbright, J. P. 2002, AJ, 123, 404

Fusi Pecci, F., Bellazzini, M., Cacciari, C. & Ferraro F. R. 1995, AJ, 110, 1664

Fusi Pecci, F., Bellazzini, M., Ferraro, F. R., Buonanno, R., & Corsi, C. E. 1996, Formation of the Galactic Halo...Inside and Out, ASP Conf. 92, eds. Morrison, H. L. & Sarajedini, A., 221

Gallart, C., Zoccali, M., & Aparicio, A. 2005, ARA&A, 43, 387

Girardi, L., & Salaris, M. 2001, MNRAS, 323, 109

Girardi, L., Bressan, A., Bertelli, G., & Chiosi, C. 2000, A&AS, 141, 371

Graham, J. A. 1975, PASP, 87, 641

Grebel, E. K. 1997, Reviews in Modern Astronomy, 10, 27

Grebel, E. K. 1999, The Stellar Content of the Local Group, IAU Symp. 192, eds. P. Whitelock & R. Cannon (San Francisco: ASP), 17

Grebel, E. K. 2001, Astrophysics and Space Science Supplement, 277, 231

Grebel, E. K., & Gallagher, J. S., III 2004, ApJ, 610, L89

Harbeck, D., et al. 2001, AJ, 122, 3092

Harris, W. E. 1996, AJ, 112, 1487

Held, E. V., Clementini, G., Rizzi, L., Momany, Y., Saviane, I., & Di Fabrizio, L. 2001, ApJ, 562, L39

Hill, V., François, P., Spite, M., Primas, F., & Spite, F. 2000, A&A, 364, L19

Iben, I. J., & Faulkner, J. 1968, ApJ, 153, 101

Johnson, J. A. Bolte, M., Stetson, P. B., Hesser, J. E., & Somerville, R. S. 1999, ApJ, 527, 199

Johnson, J. A., Bolte, M., Hesser, J. E., Ivans, I. I., & Stetson, P. B. 2004, Abundances in LMC and SMC Globular Clusters, eds. A. McWilliam & M. Rauch (Pasadena: Carnegie Observatories)

Johnson, J. A., Ivans, I. I., & Stetson, P. B. 2006, ApJ, 640, 801

Koch, A., Grebel, E. K., Gilmore, G. F., Wyse, R. F. G., Kleyna, J. T., Harbeck, D., Wilkinson, M. I., & Evans, N. W. 2007, AJ, submitted

Koekemoer, A. M., Fruchter, A. S., Hook, R. N., & Hack, W. 2002, in *Hubble* after the Installation of the ACS and the NICMOS Cooling System, eds. S. Arribas, A. Koekemoer & B. Whitmore (Baltimore: STScI), 337

Krauss, L. M., & Chaboyer, B. 2003, Science, 299, 65

Lee, Y.-W., Demarque, P., & Zinn, R. 1994, ApJ, 423, 248

Mackey, A. D. & Gilmore, G. F. 2004, MNRAS, 352, 153

Makarova, L. N., et al. 2002, A&A, 396, 473

Mighell, K. J., Sarajedini, A., & Frenck, R. S. 1998, AJ, 116, 2395

Moore, B., Diemand, J., Madau, P., Zemp, M., & Stadel, J. 2006, MNRAS, 368, 563

O'Donnell, J. E. 1994, ApJ, 422, 158

Olsen, K. A. G., Hodge, P. W., Mateo, M., Olszewski, E. W., Schommer, R. A., Suntzeff, N. B., & Walker, A. R. 1998, MNRAS, 300, 665

Olszewski, E. W., Suntzeff, N. B. & Mateo, M. 1996, ARA&A, 34, 511

Pietrinferni, A., Cassisi, S., Salaris, M., & Castelli, F. 2004, AJ, 612, 168

Piotto, G., Bedin, L. R., Anderson, A., King, I. R., Cassisi, S., Milone, A. P., Villanova, S., Pietrinferni, A. & Renzini, A. 2007, ApJ, 661, L53

Pritzl, B. J., Armandroff, T. E., Jacoby, G. H., & Da Costa, G. S. 2005, AJ, 129, 2232

Pritzl, B. J., Venn, K. A., & Irwin, M. I. 2005, AJ, 130, 2140

Ratnatunga, K. U., & Bahcall, J. N. 1985, ApJS, 59, 63

Rosenberg, A., Saviane, I., Piotto, G., & Aparicio, A. 1999, AJ, 118, 2306

Rutledge, G. A., Hesser, J. E., Stetson, P. B., Mateo, M., Simard, L., Bolte, M., Friel, E. D., & Copin, Y. 1997, PASP, 109, 883

Salaris, M., & Girardi, L. 2002, MNRAS, 337, 332

Salaris, M., & Weiss, A. 2002, A&A, 388, 492

Sarajedini, A. 1997, AJ, 113, 682

Sarajedini, A., Geisler, D., Harding, P., & Schommer, R. 1998, ApJ, 508, L37

Sarajedini, A., et al. 2002, ApJ, 567, 915

Schlegel, D. J., Finkbeiner, D. P., & Davis, M. 1998, ApJ, 500, 525

Shara, M. M., Fall, S. M., Rich, R. M., & Zurek, D. 1998, AJ, 508, 570

Shetrone, M. D., Côté, P., & Sargent, W. L. W. 2001, ApJ, 548, 592

Sirianni, M., et al. 2005, PASP, 117, 1049

Storm, J., Carney, B. W., Gieren, W. P., Fouqué, P., Latham, D. W., & Fry, A. M. 2004, A&A, 415, 531

Stryker, L. L., Da Costa, G. S. & Mould, J. R. 1985, ApJ, 298, 544

Thackeray, A. D. 1958, MNRAS, 118, 117

Udalski, A. 1998, Acta Astronomica, 48, 383

VandenBerg, D. A. 2000, ApJS, 129, 315

VandenBerg, D. A., Swenson, F. J., Rogers, F. J., Iglesias, C. A., & Alexander, D. R. 2000, ApJ, 532, 430

Walker, A. R. 1989, PASP, 101, 570

Walker, A. R. 1991, The Magellanic Clouds, IAU Symp. 148, eds. R. Haynes & D. Milne (Los Angeles: ASP), 307

Walker, A. R. 1992, ApJ, 390, L81

Zinn, R., & West, M. J. 1984, ApJS, 55, 45

Zinn, R. 1993, The Globular Cluster-Galaxy Connection, ASP Conf. Ser. 48, eds. Smith, G. H. & Brodie, J. P. (San Francisco: ASP), 302